

OMMYDCLD: A New A-Train Cloud Product that Co-Locates OMI and MODIS Cloud and Radiance Parameters onto the OMI Footprint

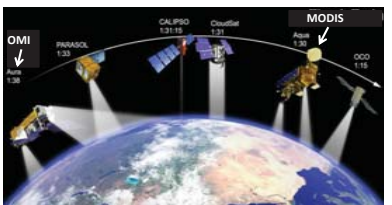
Brad Fisher¹, Joanna Joiner², Alexander Vasilkov¹, Pepijn Veefkind³, Steven Platnick², and Galina Wind¹

¹Science Systems Applications, Inc. (SSAI) ²NASA Goddard Space Flight Center, ³Royal Netherlands Meteorological Institute (KNMI)

INTRODUCTION

Clouds cover approximately 60% of the earth's surface. When obscuring the satellite's field of view (FOV), clouds complicate the retrieval of ozone, trace gases and aerosols from data collected by earth observing satellites. Cloud properties associated with optical thickness, cloud pressure, water phase, drop size distribution (DSD), cloud fraction, vertical and areal extent can also change significantly over short spatio-temporal scales. The radiative transfer models used to retrieve column estimates of atmospheric constituents typically do not account for all these properties and their variations. The OMI science team is preparing to release a new data product, OMMYDCLD, which combines the cloud information from sensors on board two earth observing satellites in the NASA A-Train: Aura/OMI and Aqua/MODIS. OMMYDCLD co-locates high resolution cloud and radiance information from MODIS onto the much larger OMI pixel and combines it with parameters derived from the two other OMI cloud products: OMCLDRR and OMCLD02. The product includes histograms for MODIS scientific data sets (SDS) provided at 1 km resolution. The statistics of key data fields – such as effective particle radius, cloud optical thickness and cloud water path – are further separated into liquid and ice categories using the optical and IR phase information. OMMYDCLD offers users of OMI data cloud information that will be useful for carrying out OMI calibration work, multi-year studies of cloud vertical structure and the identification and classification of multi-layer clouds.

NASA A-Train



This merged product takes advantage of the synergy between OMI and MODIS, which both fly on satellites in the NASA A-Train. The A-Train consists of a constellation of Earth-observing satellites that follow similar orbital tracks and collect near-simultaneous observations as shown in the above figure. Aqua leads Aura by about 8 minutes.

MODIS Collection 6

OMMYDCLD will provide users with MODIS Collection 6 cloud parameters co-located onto the OMI pixel. The recent release of Collection 6 incorporates many improvements to the retrieval of cloud information, including:

- Improved resolution to 1 km x 1 km (from 5 km x 5 km) for most cloud fields, greatly increasing the sampling statistics inside the OMI pixel
- Refinements to the spectral response functions to significantly improve the sensitivity of the cloud slicing algorithm, resulting in more frequent detection of mid to high level clouds
- Refinements to the approach for determining low-level cloud height over oceans using the 11 μm channel
- Application of various independent tests for the existence of multi-level clouds (Baum et al. 2012).

Instrument Overview

Instruments

- Ozone Monitoring Instrument (OMI)
 - Hyperspectral Imager: UV1: 270 to 314 nm, UV2: 306 to 380 nm, VIS: 350 to 500 nm
- MODerate-resolution Imaging Spectroradiometer (MODIS)
 - 36 spectral bands ranging from 0.4 to 14.4 μm

Spatial Coverage

- OMI swath width: 2600 km
- MODIS swath width: 2300 km
- MODIS overlap of OMI covers rows 4 to 60 along OMI's X-track

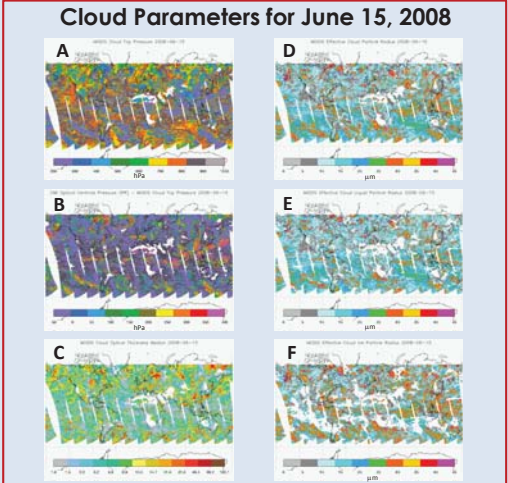
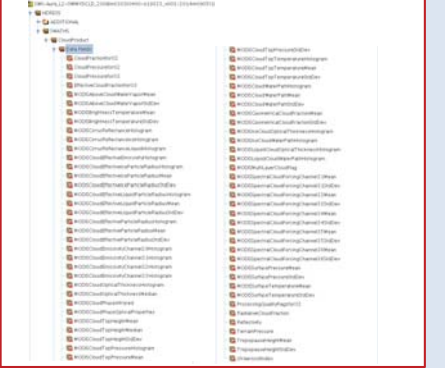
Field of View

- OMI UV2: 13 x 24 km² for row 30, 28 x 150 km² for row 60
- MODIS: 1 x 1 km² and 5 x 5 km² (depending on the SDS)

MODIS Sampling of OMI pixel

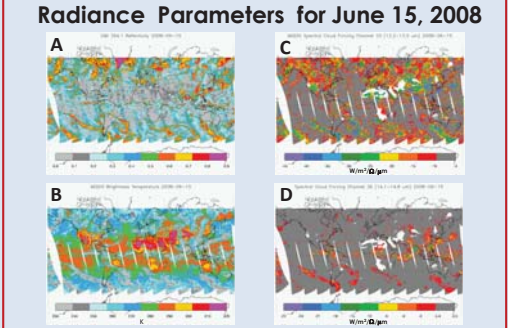
- At 1 km: ~300 for row 30, ~700 for row 60
- At 5 km: ~12 for row 30, ~30 for row 60

OMMYDCLD Atmospheric Parameters



The six images shown above display cloud parameters from OMMYDCLD for a full day of OMI orbits for June 15, 2008. These images show product samples for A) MODIS Cloud Top Pressure, B) OMI Cloud RR - MODIS Cloud Top Pressure, C) MODIS Cloud Optical Depth (median), D) MODIS Effective Particle Radius, E) Effective Liquid Particle Radius, and F) Effective Ice Particle Radius.

The retrieval of cloud optical thickness (τ_c) and effective particle radius (r_e) by MODIS computes the inverse of the integrated reflections function, in which the solar reflection and earth emission components of the measured radiation are separated. Non-absorbing solar visible bands are used to retrieve τ_c , whereas absorbing near IR bands are used to retrieve r_e . The dark grey areas in B) represent pixels where the effective cloud fraction < 0.20.



The four images shown above display radiance parameters for June 15 2008. The radiance fields shown include A) OMI Reflectivity at 354.1 nm, B) MODIS Brightness Temperature, C) MODIS Spectral Cloud Forcing (SCF) for Channel 33 (13.2-13.5 μm) and D) MODIS Spectral Cloud Forcing for Channel 36 (14.1-14.5 μm). Channels 33 and 36 are involved in the cloud slicing algorithm. The weighting function for channel 33 peaks at 900 hPa, while channel 36 peaks at 300 hPa. The high clouds, some of which are deep convective clouds in the tropics, are seen clearly in D).

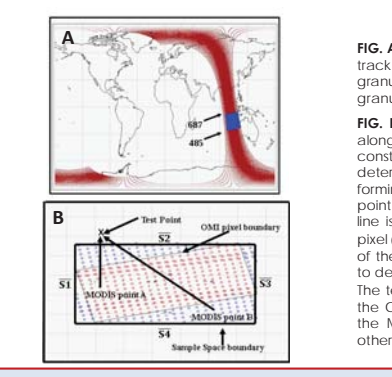
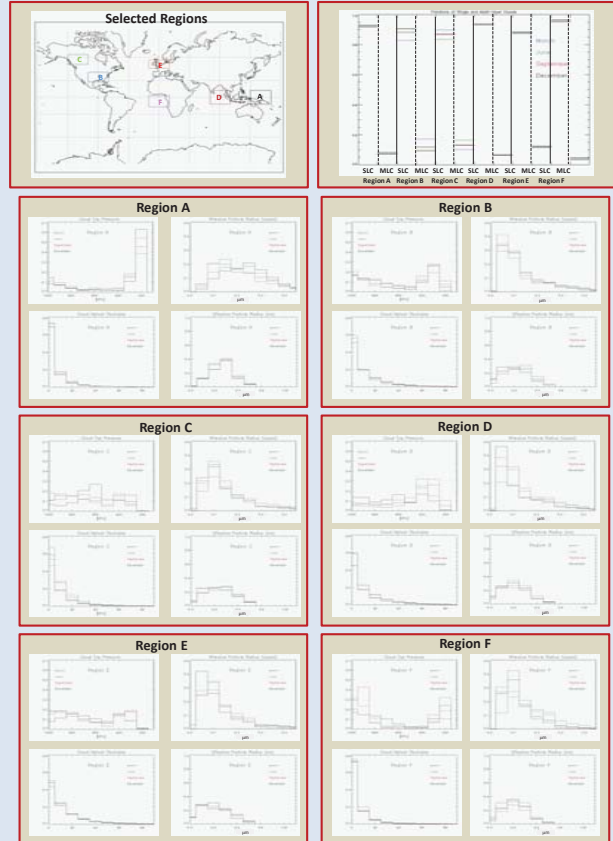


FIG. A: MODIS Granules span a 5-minute interval along the OMI orbital track. A typical OMI orbit (red) is shown with overlapping 5-min MODIS granule (blue). About 200 OMI scan lines are processed per MODIS granule.

FIG. B: An OMI pixel and a corresponding Sample Space – defined along constant latitudinal and longitudinal boundaries – are constructed using the OMI pixel corner product OMIPIXCOR. To determine if a MODIS pixel is inside the OMI pixel – constructed by forming straight lines between pixel corners (i.e., S1, S2, S3, S4) – a test point (X) is arbitrarily selected just outside of the Sample Space and a line is defined between the test point and the center of the MODIS pixel (i.e., \overline{AX} , \overline{BX}). Linear equations are subsequently defined for each of the four OMI pixel boundaries. A "line crossing test" is then applied to determine if the MODIS pixel falls inside of the OMI pixel boundaries. The test counts the number of intersections between \overline{AX} (or \overline{BX}) and the OMI pixel boundaries. If the number of intersections is odd, then the MODIS pixel is inside the OMI pixel boundaries (shown in red), otherwise it is outside (shown in blue).



Daily histograms of selected MODIS SDS were generated from OMMYDCLD using a test data set at a resolution of 30° longitude x 5° latitude. For this analysis, we considered cloud top pressure, cloud optical thickness, single and multi-layer clouds (SLC and MLC) and effective particle radius (liquid and ice), based on four months of data (March, June, September and December). The daily histograms were then further aggregated into monthly histograms for the six regions shown in the above map, labeled A, B, C, D, E and F. The results of this analysis are shown in the six panels above, labeled by region. Note that in computing the fractions of SLC and MLC, all seven confidence levels from the MODIS multi-layer cloud field were summed up for the MLC to provide a single number and then normalized with respect to the SLC. MODIS only provides one bin for the SLC.

REFERENCES

- Joiner, J., Vasilkov, A. P., Gupta, P., Bharila, P. K., Veefkind, P., Sreep, M., de Haan, J., Polonsky, L. and Spurr, R. 2012: Fast simulator for satellite cloud optical centroid pressure retrieval; evaluation of OMI cloud retrievals. Atmos. Meas. Tech., 5, 529-545, doi:10.5194/amt-5-529-2012.
- Joiner, J., Vasilkov, A. P., Bharila, P. K., Wind, G., Platnick, S. and W. P. Menzel, 2010: Detection of multi-layer and vertically-extended clouds using A-train sensors. Atmos. Meas. Tech., 3, 233-247.
- Sreep, M., J. F. de Haan, P. Stammes, P. Wang, C. Vanbauc, J. Joiner, A. P. Vasilkov, and P. F. Levelt, 2008: Three-way comparison between OMI and PARASOL cloud pressure products. J. Geophys. Res., 113, D15523, doi:10.1029/2007JD008694.
- Platnick, S., M. D. King, S. A. Ackerman, W. P. Menzel, B. A. Riedi and R. A. Frey, 2003: The MODIS cloud products: algorithms and examples from Terra. IEEE, 41, Issue 2, pp. 459 - 473.
- Vasilkov, A. P., J. Joiner, R. Spurr, P. K. Bharila, P. F. Levelt, and G. Stephens, 2008: Evaluation of the OMI cloud pressures derived from rotational Raman scattering by comparisons with satellite data and radiative transfer simulations. J. Geophys. Res., 113, D15519, doi:10.1029/2007JD008689.
- Baum, B. A., W. P. Menzel, R. A. Frey, D. C. Tobin, R. E. Holz, S. A. Ackerman, A. K. Heidinger and P. Yang, 2012: MODIS cloud-top-property refinements for Collection 6. JAMC, 51, 1145-1163.